International Journal on Magnetic Particle Imaging
Vol 10, No 1, Suppl 1, Article ID 2403017, 4 Pages

Infinite Science Publishing

Proceedings Article

Magnetic particle imaging can be used to assess tumour associated macrophage density in vivo

Nitara Fernando [a,b,*] · Julia Gevaert [a,b] · Paula Foster [a,b]

[a] Robarts Research Institute, London, Ontario, Canada
[b] The Department of Medical Biophysics, Western University, London, Ontario, Canada
[*] Corresponding author, email: nferna47@uwo.ca

Abstract

Tumour Associated Macrophages (TAMs) play a crucial role in breast cancer prognosis. Here we propose Magnetic Particle Imaging (MPI) for non-invasive TAM assessment. By employing an advanced reconstruction algorithm and a small field of view (FOV) focused on the tumour, we demonstrate enhanced image quality and successful quantification of TAMs in mouse mammary tumours with different metastatic potentials (4T1 and E0771). Utilizing in vivo MPI, we did not see significant differences in the MPI signal for 4T1 tumours compared to E0771. These findings highlight the potential of MPI for in vivo TAM quantification despite dynamic range limitations, offering a promising avenue for broader applications in cancer research and potentially overcoming constraints in other in vivo imaging contexts.

I. Introduction

Tumour associated macrophages (TAMs) are a highly prevalent component of the tumour microenvironment (TME), and they can constitute up to 50% of the breast cancer TME [1]. In breast cancer, higher TAM infiltration has been associated with poorer patient prognosis [1–3] . TAM density is usually assessed using immunohistochemistry (IHC); however, this requires invasive biopsies and is not representative of the whole tumour [4]. Thus, there is a need for non-invasive and quantitative imaging that allows for the in vivo assessment of TAMs, which could serve as a biomarker for tumour aggressiveness.

Superparamagnetic iron oxide (SPIO) particles can be used to label macrophages in situ via an intravenous (IV) injection and this approach has been used for imaging TAMs with MRI [5–7]. However, quantification of TAM density from iron-induced signal loss in MRI is challenging. Magnetic Particle Imaging (MPI) is emerging as an in vivo cellular imaging method and can provide measurements of iron mass which allow us to estimate cell number from images. MPI has previously been evaluated for TAM cell tracking; however, quantification was only possible for fixed tumour tissues imaged ex vivo due to known dynamic range limitations [8]. When iron samples with large differences in concentrations are present in the same field of view (FOV) there is signal oversaturation from the higher signal due to the requirement for regularization for stable reconstruction. The high uptake of SPIO in liver macrophages after IV injection prevented isolation of the lower TAM signal. This represents a major roadblock for in vivo MPI in applications where two or more sources of signal exist. This was recently demonstrated for quantifying the migration of dendritic cells to the popliteal lymph node (small signal) after their injection into the mouse footpad (large signal) [9].

This limitation can be addressed by using a small FOV focused on the tumour, together with an advanced reconstruction algorithm. In 2015, Konkle et al. introduced an advanced reconstruction method which employs a priori information, non-negativity, and image smoothness to enhance image quality [10].

Here, we evaluate the use of a small, focused FOV and the advanced reconstruction method first using samples of iron, where a sample with a high iron concentration is positioned 2 cm away from a sample with a much lower iron concentration and show that this approach removes image artifacts seen in the native MPI reconstruction. Then, we employ this strategy for quantitative imaging of tumours in vivo after IV SPIO and compare the MPI signal for mouse mammary tumours induced using two breast cancer cell lines with different metastatic potentials.

II. Methods and Materials

MPI Image Reconstruction: All experiments were performed using the Momentum™ pre-clinical MPI scanner (Magnetic Insight Inc.). The native image reconstructions are formed by the X-space stitching method [10, 11]. In this method the panels of data are stitched together and the edges of the image are pinned to zero, which allows for the recovery of the filtered DC component.

To acquire the images using the advanced reconstruction, we enabled the 'inverse_xz_image_combiner' option in the MOMENTUM Advanced User Interface. This option reconstructs native images using x-space methods as described above and applies an inverse problem postprocessing step. The postprocessing combines native images that were reconstructed separately depending on the direction of transmit (positive and negative), sharpens using the equalized PSF [12], and corrects the edge-pinning applied in the native image reconstruction step. The postprocessing is formulated as a matrix-free non-negative least squares inverse problem and is solved using FISTA as in previous formulations [10].

In vitro assessment of advanced reconstruction: A 780 ng Fe sample was placed 2 cm apart from a 50 μg Fe sample and MPI was repeated with triplicate samples. A 2 cm FOV was centered on the 780 ng sample and images were acquired for each sample (n=3) using the standard native reconstruction algorithm and the advanced reconstruction algorithm. Images were acquired with a 3.0 T/m selection field gradient and drive field strength of –23mT (z).

Animals: BALB/c and C57BL/6 mice were purchased from Charles River Laboratories, Inc. (Senneville, CAN). All animal studies were performed in accordance with institutional and national guidelines.

Tumour Models: 4T1 and E0771 mouse breast cancer cell lines (100,000 cells, 50 μL injection volume) were administered subcutaneously to the fourth mammary fat pad of C57BL/6 mice (E0771, n=8) and BALB/c mice (4T1, n=8). E0771 is poorly metastatic compared to 4T1 [13].

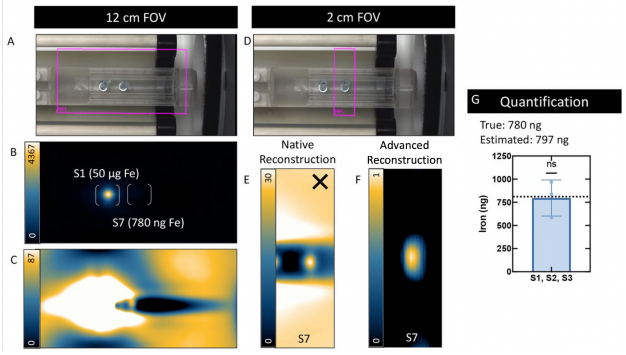

Figure 1: Small FOV imaging with advanced reconstruction as a solution for quantifying two proximal samples with varying iron mass. (A) Experimental set-up showing the full 12 cm FOV around a source of low iron signal (S7, 780 ng Fe) 2 cm apart from a higher iron signal (S1, 50 μg Fe). (B) In Full dynamic range, only signal coming from the higher iron sample (S1) is visible. (C) Window leveling to the minimum and maximum signal of the lower signal (S7) oversaturates the high signal and prevents quantification of S7. (D) A 2 cm FOV centered on the low sample (S7) and acquired with (E) native reconstruction, which did not quantify signal and (F) advanced reconstruction, which did quantify signal. (G) The advanced reconstruction successfully isolated the low signal and average iron content was estimated to be 797 ng Fe for triplicate samples, consistent with known iron content (780 ng Fe) ($p > 0.05$).

MPI Imaging: Twenty days after the cell injection, 30mg/kg of a SPIO (Synomag-D-PEG, Micromod GmbH) was administered IV to mice and 24 hours later imaging was performed using the Momentum™ scanner (Magnetic Insight, Inc.). Images were acquired with a 5.7 T/m selection field gradient and drive field strength of -23mT (z). Tumours were imaged with the native reconstruction and a 12 (z) x 6 (x) cm FOV, and the advanced reconstruction with a 3 (z) x 6 (x) cm FOV. Total MPI signal and average iron per tumour were measured using an open-source medical imaging viewer (Horos v4.0.0 RC5). Mice were euthanized and tumours were removed for ex vivo MPI imaging.

III. Results

MPI signal and iron content were quantified for 4T1 and E0771 tumour bearing mice. There was no significant difference in either between the two tumour types. (Figure 2E, F). Ex vivo imaging of tumours using MPI shows presence of signal in all tumours, confirming that signal observed in in vivo images is from tumours (Figure 4). Additionally, in vivo and ex vivo imaging of control tumours shows no MPI signal, as expected.

Figure 1A and D show the positioning of the 12 and 2

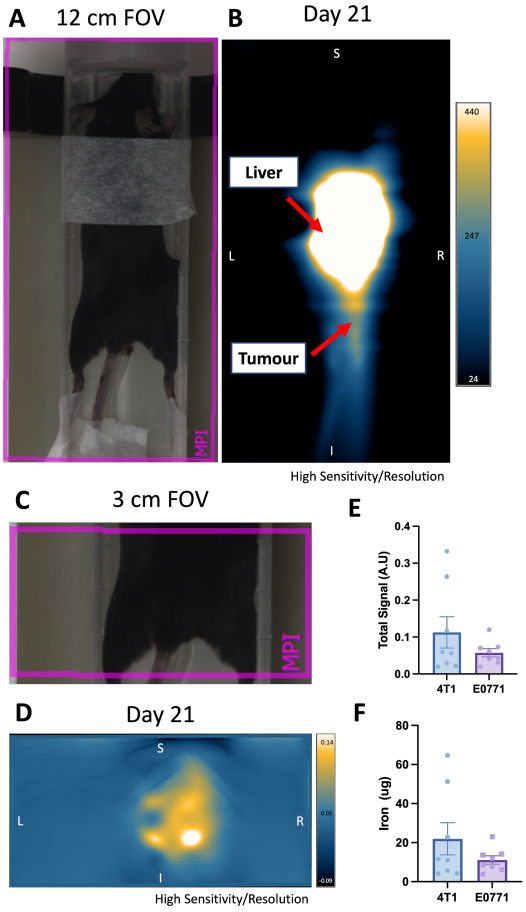

Figure 2: In vivo imaging of tumours using MPI following tail vein injection of Synomag-D PEG. The standard 12 cm FOV is shown in A by the pink box encompassing the mouse body positioned for imaging. The corresponding 2D MPI image is shown in B; the very high liver signal interferes with the detection of the tumour signal. A 3 cm FOV was be applied over the tumour region, shown by the pink box in C, allowing for isolation of tumour signal (D). The signal obtained with partial FOV imaging can be quantified as total signal (E) or iron content (F) using a previously established calibration line.

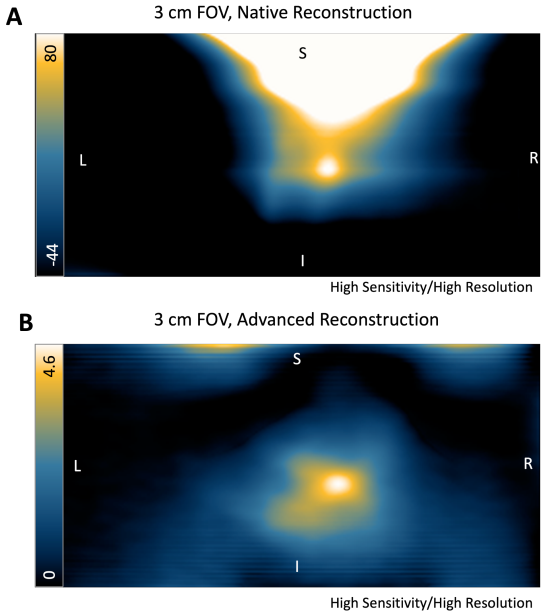

Figure 3: Native and advanced reconstruction when imaging tumours with a 3 cm FOV. (A) Despite using a small FOV, signal from liver region oversaturates tumour region and prevents quantification. (B) With the advanced reconstruction tumour signal and can isolated and quantified.

cm FOV on the iron samples (780 ng and 50 ug). With the 12 cm FOV (Figure 1B,C) isolation of the 780 ng Fe signal is not possible due to dynamic range limitations. When the image window width and level are adjusted to the maximum and minimum signal of the 780 ng sample, the higher signal (50ug) oversaturates the lower signal (780 ng). With the 2 cm FOV centered on the 780 ng sample, an artifact-free small FOV was not possible with the native MPI reconstruction, which assumes zero signal along the edges of the FOV and creates a negative signal artifact when the assumptions are not met (Figure 1E). With the advanced reconstruction (Figure 1F) the 780 ng sample can be quantified within 10% of the actual iron content (Figure 1G).

When imaging tumours with the full FOV (Figure 2A) we observed signal oversaturation from the liver region of the mouse and were unable to isolate and quantify signal from the tumour (Figure 2B). This is due to the previously described limitation in MPI dynamic range. This was solved using a FOV focused on the tumour region and the advanced reconstruction (Figure 2C,D), which allowed MPI signal to be quantified for all tumors. An example of the artifact produced when using a FOV focused on the tumour with the native reconstruction method is shown in Figure 3.

IV. Discussion

This work presents the first demonstration of in vivo imaging and quantification of TAMs using MPI. While MPI dynamic range is a known limitation, using the advanced reconstruction and small FOV we were able to isolate tumour signal and show that it can be attributed to the accumulation of iron in the tumours. Ongoing histology will be used to validate the presence of iron-positive TAMs. This work also demonstrates the potential of MPI for other in vivo applications where dynamic range can cause limitations.

10.18416/ijmpi.2024.2403017

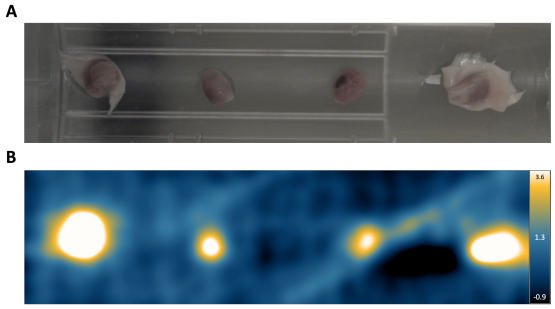

Figure 4: Ex-vivo imaging of 4T1 tumours with MPI to determine iron presence. (A) Four representative 4T1 tumours from Balb/c mice can be seen. Tumours were placed on an empty MPI bed for imaging (2D, High sensitivity isotropic). (B) Corresponding MPI signal for each tumour can be seen, with signal detected for all tumours imaged. These results confirm the presence of SPIO in the tumours.

Acknowledgments

Special thanks to Dr. Olivia Sehl for technical assistance and Stefaan Soenen [Katholieke Universiteit Leuven] for gifting the E0771 and 4T1 cells used in this study.

Author's statement

Conflict of interest: Authors state no conflict of interest. Ethical approval: The research related to animal use complies with all the relevant national regulations, institutional policies and was performed in accordance with the standards of the Canadian Council on Animal Care, under an approved protocol by the Animal Use Subcommittee of Western University's Council on Animal Care. We would also like to acknowledge funding from the Canadian Foundation for Innovation and the IMPAKT Facility at Western University.

References

[1] S. M. A. Mahmoud, A. H. S. Lee, E. C. Paish, R. D. Macmillan, I. O. Ellis, and A. R. Green. Tumour-infiltrating macrophages and clinical outcome in breast cancer. *Journal of Clinical Pathology*, 65(2):159–163, 2011.

[2] M. J. Campbell, N. Y. Tonlaar, E. R. Garwood, D. Huo, D. H. Moore, A. I. Khramtsov, A. Au, F. Baehner, Y. Chen, D. O. Malaka, A. Lin, O. O. Adeyanju, S. Li, C. Gong, M. McGrath, O. I. Olopade, and L. J. Esserman. Proliferating macrophages associated with high grade, hormone receptor negative breast cancer and poor clinical outcome. *Breast Cancer Research and Treatment*, 128(3):703–711, 2010.

[3] R. D. Leek, C. E. Lewis, R. Whitehouse, M. Greenall, J. Clarke, and A. L. Harris. Association of macrophage infiltration with angiogenesis and prognosis in invasive breast carcinoma. *Cancer Res*, 56(20):4625–4629, 1996.

[4] J. Zhou, Z. Tang, S. Gao, C. Li, Y. Feng, and X. Zhou. Tumor-associated macrophages: Recent insights and therapies. *Frontiers in Oncology*, 10, 2020, doi:10.3389/fonc.2020.00188.

[5] H. E. Daldrup-Link, D. Golovko, B. Ruffell, D. G. DeNardo, R. Castaneda, C. Ansari, J. Rao, G. A. Tikhomirov, M. F. Wendland, C. Corot, and L. M. Coussens. MRI of tumor-associated macrophages with clinically applicable iron oxide nanoparticles. *Clinical Cancer Research*, 17(17):5695–5704, 2011, doi:10.1158/1078-0432.ccr-10-3420.

[6] A. V. Makela, J. M. Gaudet, and P. J. Foster. Quantifying tumor associated macrophages in breast cancer: A comparison of iron and fluorine-based MRI cell tracking. *Scientific Reports*, 7(1), 2017, doi:10.1038/srep42109.

[7] Y.-Y. I. Shih, Y.-H. Hsu, T. Q. Duong, S.-S. Lin, K.-P. N. Chow, and C. Chang. Longitudinal study of tumor-associated macrophages during tumor expansion using MRI. *NMR in Biomedicine*, 24(10):1353–1360, 2011, doi:10.1002/nbm.1698.

[8] A. V. Makela, J. M. Gaudet, M. A. Schott, O. C. Sehl, C. H. Contag, and P. J. Foster. Magnetic particle imaging of macrophages associated with cancer: Filling the voids left by iron-based magnetic resonance imaging. *Molecular Imaging and Biology*, 22(4):958–968, 2020, doi:10.1007/s11307-020-01473-0.

[9] C. Fink, J. J. Gevaert, J. W. Barrett, J. D. Dikeakos, P. J. Foster, and G. A. Dekaban. In vivo tracking of adenoviral-transduced iron oxide-labeled bone marrow-derived dendritic cells using magnetic particle imaging. *European Radiology Experimental*, 7(1), 2023, doi:10.1186/s41747-023-00359-4.

[10] J. J. Konkle, P. W. Goodwill, D. W. Hensley, R. D. Orendorff, M. Lustig, and S. M. Conolly. A convex formulation for magnetic particle imaging x-space reconstruction. *PLOS ONE*, 10(10):e0140137, 2015, doi:10.1371/journal.pone.0140137.

[11] P. W. Goodwill and S. M. Conolly. Multidimensional x-space magnetic particle imaging. *IEEE Transactions on Medical Imaging*, 30(9):1581–1590, 2011.

[12] K. Lu and S. M. Conolly. Linearity, shift-invariance and resolution improvement for quantitative magnetic particle imaging. *UC Berkeley*, 2015.

[13] C. N. Johnstone, Y. E. Smith, Y. Cao, A. D. Burrows, R. S. N. Cross, X. Ling, R. P. Redvers, J. P. Doherty, B. L. Eckhardt, A. L. Natoli, C. M. Restall, E. Lucas, H. B. Pearson, S. Deb, K. L. Britt, A. Rizzitelli, J. Li, J. H. Harmey, N. Pouliot, and R. L. Anderson. Functional and molecular characterisation of eo771.lmb tumours, a new c57bl/6-mouse-derived model of spontaneously metastatic mammary cancer. *Disease Models & Mechanisms*, 2015.

